Inhibiting Monoacylglycerol Acyltransferase 1 Ameliorates Hepatic Metabolic Abnormalities but Not Inflammation and Injury in Mice*

Nisreen Soufi[‡§], Angela M. Hall[§], Zhouji Chen[§], Jun Yoshino[§1], Sara L. Collier[§], James C. Mathews[¶], Elizabeth M. Brunt[¶], Carolyn J. Albert[∥], Mark J. Graham[**], David A. Ford[∥], and Brian N. Finck[§2]

From the Departments of [‡]Pediatrics, [§]Medicine, and [¶]Pathology and Immunology, Washington University School of Medicine, Saint Louis, Missouri 63110, the [∥]Edward A. Doisy Department of Biochemistry and Molecular Biology, Saint Louis University School of Medicine, Saint Louis, Missouri 63104, and [**]ISIS Pharmaceuticals Inc., Carlsbad, California 92008

Background: *Mogat1* inhibition improves glucose metabolism in obese mice, but its effects on liver injury are unknown.
Results: *Mogat1* knockdown improved hepatic metabolic abnormalities but did not reduce liver inflammation or injury.
Conclusion: Hepatic injury and metabolic abnormalities are separable disease entities.
Significance: Attention to liver injury markers should be made when evaluating metabolic therapies.

Abnormalities in hepatic lipid metabolism and insulin action are believed to play a critical role in the etiology of nonalcoholic steatohepatitis. Monoacylglycerol acyltransferase (MGAT) enzymes convert monoacylglycerol to diacylglycerol, which is the penultimate step in one pathway for triacylglycerol synthesis. Hepatic expression of *Mogat1*, which encodes an MGAT enzyme, is increased in the livers of mice with hepatic steatosis, and knocking down *Mogat1* improves glucose metabolism and hepatic insulin signaling, but whether increased MGAT activity plays a role in the etiology of nonalcoholic steatohepatitis is unclear. To examine this issue, mice were placed on a diet containing high levels of trans fatty acids, fructose, and cholesterol (HTF-C diet) or a low fat control diet for 4 weeks. Mice were injected with antisense oligonucleotides (ASOs) to knockdown *Mogat1* or a scrambled ASO control for 12 weeks while remaining on diet. The HTF-C diet caused glucose intolerance, hepatic steatosis, and induced hepatic gene expression markers of inflammation, macrophage infiltration, and stellate cell activation. *Mogat1* ASO treatment, which suppressed *Mogat1* expression in liver and adipose tissue, attenuated weight gain, improved glucose tolerance, improved hepatic insulin signaling, and decreased hepatic triacylglycerol content compared with control ASO-treated mice on HTF-C chow. However, *Mogat1* ASO treatment did not reduce hepatic diacylglycerol, cholesterol, or free fatty acid content; improve histologic measures of liver injury; or reduce expression of markers of stellate cell activation, liver inflammation, and injury. In conclusion, inhibition of hepatic *Mogat1* in HTF-C diet-fed mice improves hepatic metabolic abnormalities without attenuating liver inflammation and injury.

Nonalcoholic fatty liver disease (NAFLD)[3] is one of the most common types of chronic liver disease. NAFLD is extremely prevalent in obese individuals, and rates of NAFLD are rising with the increased incidence of obesity. The term "NAFLD" encompasses a spectrum of disorders that ranges from simple steatosis to steatohepatitis (NASH) and cirrhosis, although only a small percentage of patients with NAFLD are classified to have NASH (1). Moreover, it is not clear whether simple steatosis progresses to NASH or whether these are two separate entities. Several genetic, dietary, and environmental factors have been implicated as risk factors for NASH (2–4). In addition, evidence has emerged that hepatic insulin resistance and inflammation, probably caused by accumulation of toxic lipids, may play a role in the development and progression of NASH. However, much remains unclear regarding the pathogenic mechanisms of NASH development, and the dynamic interplay among abnormal intermediary metabolism, insulin resistance, inflammation, and liver injury is unclear.

The hallmark of NAFLD is accumulation of neutral lipids, primarily triacylglycerol (TAG) by mass, in hepatocytes. Mammalian cells synthesize TAG by two convergent pathways: the glycerol-3-phosphate and the monoacylglycerol acyltransferase (MGAT) pathways. MGAT enzymes catalyze the acylation of MAG to DAG, which is the direct precursor of TAG. In higher organisms, a family of three related genes (*Mogat1*, *Mogat2*, and *Mogat3*) encoding enzymes with MGAT activity has been identified, but the mouse *Mogat3* is a pseudogene (5).

MGATs have been most thoroughly studied in intestinal enterocytes, where they play important roles in mediating dietary fat absorption and chylomicron secretion (6, 7). MGAT activity may also be important for TAG recycling by re-esterifying fatty acids to lipolytic remnants (8, 9).

MGAT activity in human liver is substantial (10), and MGAT expression is strikingly increased in NAFLD (10–13). Previous work using antisense oligonucleotides (ASOs) and RNAi approaches have shown that short term hepatic suppression of *Mogat1* led to a significant improvement in hepatic insulin signaling and whole-body glucose homeostasis (12, 13). The improved glucose tolerance after ASO-mediated knockdown was associated with improved insulin signaling in liver but not other tissues and was not associated with enhanced insulin secretion (13). Although both previous studies demonstrated a profound insulin-sensitizing effect, neither study examined markers of liver injury, inflammation, or fibrosis after knockdown of *Mogat1*.

In this study, we characterized the transcriptional effects of inhibiting *Mogat1* in diet-induced obese (DIO) mice. The surprising finding was that *Mogat1* knockdown by ASO for 3 weeks actually exacerbated expression of markers of oxidative stress and inflammatory signaling in mice with marked improvements in glucose homeostasis and hepatic insulin signaling. Therefore, we also evaluated the effects of prolonged inhibition of *Mogat1* in liver and adipose tissue by ASO injection in a mouse model of NASH provoked by feeding a diet enriched with trans fat, fructose, and cholesterol (14, 15). Suppression of hepatic and adipose tissue *Mogat1* attenuated weight gain, reduced hepatic TAG content, and markedly improved glucose tolerance in mice fed this diet. However, *Mogat1* inhibition ultimately did not reduce hepatocyte ballooning, NAFLD scoring, or expression of gene markers of inflammation, macrophage infiltration, and stellate cell activation. These data suggest a disconnect between the beneficial metabolic effects of *Mogat1* inhibition, hepatic inflammation, and the pathogenesis of NASH in a mouse model. This study also aids in the understanding of the difference between the benign entity of fat accumulation in the liver and hepatic injury, inflammation, and fibrosis.

EXPERIMENTAL PROCEDURES

Animal Study Design—For data shown in Fig. 1, C57BL/6J male mice were fed chow providing 60% of calories from fatty acids (D12492, Research Diets Inc.) starting at 6 weeks of age. Age-matched mice were maintained on a matched 10% fat chow (D12450B, Research Diets Inc.). Mice received intraperitoneal injections of ASO directed against *Mogat1* or a scrambled control ASO (25 mg/kg body weight; ISIS Pharmaceuticals, Carlsbad, CA) twice a week for 3 weeks. Treatments were initiated after 14 weeks of high fat diet feeding as described (13). Mice were sacrificed after 3 weeks of injections with ASOs, and tissues were harvested, frozen in liquid nitrogen, and stored at −80° for further analyses.

In a second study, 7-week-old C57BL/6J male mice purchased from Jackson Laboratories (Bar Harbor, ME) were placed on a diet enriched with fat (40% kcal, mainly trans fat; *trans*-oleic and *trans*-linoleic acids), cholesterol (2% weight),

TABLE 1
HTF-C and control LF diet composition

Diet#	D09100301 HTF-C		D09100304 LF	
	gm%	Kcal%	gm%	Kcal%
Protein	22.5	20	19.2	20
Carbohydrate	44.9	40	67.3	70
Fat	19.9	40	4.3	10
Total		100		100
Kcal/gm	4.49		3.85	
Ingredient	gm	Kcal	gm	Kcal
Caseine	200	800	200	800
L- Cystine	3	12	3	12
Corn Starch	0	0	350	1400
Maltodextrin 10	100	400	85	340
Fructose	200	800	0	0
Glucose	0	0	169	676
Sucrose	96	384	96	385
Cellulose BW200	50	0	50	0
Soybean oil	25	0	50	0
Primex shortening	135	1215	0	0
Lard	20	180	20	180
Cholesterol	18	0	0	0
Mineral Mix S10026	10	0	10	0
DiCalcium Phosphate	13	0	13	0
DiCalcium Carbonate	5.5	0	5.5	0
Potassium Citrate, H2O	16.5	0	16.5	0
Vitamin Mix	10	40	10	40
Choline Bitartrate	2	0	2	0
Dye	0.5	0	0.5	0
Total	904.5	4056	1055.5	4057

and fructose (22% weight) (HTF-C diet) (D09100301 Research Diets Inc.) that has been described to cause hepatic injury and inflammation (14). Age- and strain-matched mice were fed a matched low fat (10% kcal) control diet that was not supplemented with fructose or cholesterol (LF diet) (D09100304, Research Diets Inc.). Diet compositions can be found in Table 1. After remaining on the designated diets for 4 weeks, the mice received intraperitoneal injections of ASO directed against *Mogat1* or scrambled control ASO (25 mg/kg body weight; ISIS Pharmaceuticals, Carlsbad, CA). Injections were given twice a week for 2 weeks and then once a week for 10 weeks. Body weight was checked weekly. Mice were sacrificed, and tissues were harvested at the end of week 16 of the study after a 4-h fast. Liver, gonadal, and subcutaneous fat tissue samples were frozen in liquid nitrogen and stored at −80 °C. Animal studies were approved by the institutional animal use and care committees of Washington University School of Medicine and fulfilled National Institutes of Health requirements for humane care.

Glucose Tolerance Test—At week 14 of the study, two mice were fasted for 6 h and then injected with a 10% D-glucose solution (1 g/kg). Tail blood glucose was measured at 0, 30, 60, and 120 min after injection using a One-Touch Ultra glucometer (Life Scan, Inc.). Total area under the curve was calculated using the trapezoidal rule.

Hepatocyte Isolation and Metabolic Studies—Primary mouse hepatocytes were isolated and cultured as described previously (16). All metabolic experiments were carried out 4–5 h after the hepatocytes were plated. Palmitate oxidation rates were assessed using [^{3}H]palmitate as described previously (16, 17). *De novo* lipogenesis was measured by determining the incorporation rate of [^{14}C]acetate in cellular fatty acids following a 2-h incubation period (18). TAG synthesis rates were quantified by using [^{3}H]glycerol in the presence of 0.2 mM BSA-conjugated oleic acid as described previously (19), and TAG turnover was estimated by counting the intracellular [^{3}H]TAG content 14 h after [^{3}H]glycerol pulse.

Western Blot Analyses of Insulin Signaling—After a 4-h attachment period, hepatocytes were incubated in serum-free DMEM for 1 h. Protein extracts were obtained from hepatocytes 5 min after stimulation with 100 nM insulin. Antibodies to Akt, Ser(P)-473 Akt, and Thr(P)-308 Akt (Cell Signaling, Danvers, MA) or tubulin (Sigma) were used according to the manufacturer's instructions for Western blotting analyses.

mRNA Isolation and Quantitative RT-PCR—Total liver mRNA was extracted with RNA Bee (Isotex Diagnostics, Friendswood, TX) based on the manufacturer's instructions. cDNA was synthesized using Vilo reagents. Quantitative real-time PCR was performed with Power SYBR Green and using an ABI PRISM 7500 sequence detection system (Applied Biosystems, Foster City, CA). Arbitrary units of mRNA of the genes of interest were corrected to the level of the 36B4 mRNA quantified by using $\Delta/\Delta C_t$. Primers were obtained through Integrated DNA Technologies (Coralville, IA). The sequences of primers used in this paper are available upon request.

Microarray Study and Pathway Analysis—Total liver mRNA was used for Illumina Mouse 6 whole microarrays (version 2). Parametric analysis of gene set enrichment was performed as described previously (20, 21). In brief, gene sets were obtained from the Molecular Signatures Database (gene ontology gene sets, C5 collection), and Z scores and p values were calculated for each gene set. A p value of <0.05 was considered significantly changed. All data were analyzed by the R statistical software package (available at the Bioconductor Web site). All microarray data used in this study have been deposited into the NCBI GEO database (accession number GSE60349).

Histology—Harvested liver tissue samples for histology were fixed in 10% formalin for 24 h and then embedded in paraffin. Sections of the samples were stained by hematoxylin and eosin (H&E) and Mason's trichrome stains and assessed by a single pathologist blinded to the groups to which the samples belonged. Specific histological features (steatosis, inflammation, hepatocyte ballooning, and fibrosis) were evaluated and scored according to NAFLD activity score (NAS) (22, 23). Steatosis grading was done on low to medium power evaluation of parenchymal involvement by steatosis (0 for <5%, 1 for 5–33%, 2 for 33–66%, and 3 for more than 66%). Inflammation was graded by overall assessment of all inflammatory foci on a $\times200$ field (0 for no foci, 1 for <2, 2 for 2–4 foci, and 3 for >4 foci). The ballooning score was 0 for no ballooned cells per field, 1 for few, and 2 for many. Fibrosis was graded 0 for no fibrosis, 1 for perisinusoidal or periportal/portal, 2 for perisinusoidal and periportal/portal, 3 for bridging fibrosis, and 4 for cirrhosis. NAS is the sum of steatosis, inflammation, and ballooning scores.

Plasma Aspartate Aminotransferase (AST) and Alanine Aminotransferase (ALT) Concentrations—Plasma AST and ALT concentrations were measured by using a commercially available colorimetric kinetic assay (Teco Diagnostics, Anaheim, CA) and plasma collected at sacrifice.

Tissue Lipid Measurement—Hepatic TAG content was measured after homogenizing the liver samples in PBS, solubilizing the lipids in the samples by adding 100 μl of 1% sodium deoxycholate to 100 μl of the liver homogenate, and then incubating for 5 min at 37 °C. The TAG content was then determined using an enzymatic assay kit from Thermo Scientific following the manufacturer's instructions. DAG, free cholesterol, and free fatty acid (FFA) content was determined by mass spectrometry as described previously (24–26).

Statistical Analyses—Results are presented as the means $\pm$ S.E. Statistical significance was calculated using an unpaired Student's t test, with a statistically significant difference defined as a p value of ≤0.05.

RESULTS

Improvements in Glucose Homeostasis in Diet-induced Obese Mice by Mogat1 Knockdown Are Associated with Enhanced Hepatic Inflammation—We have recently shown that ASO-mediated knockdown of *Mogat1* in mice fed a 60% fat diet markedly improves hepatic insulin signaling and systemic glucose metabolism (13). To further characterize the *Mogat1* inhibition-induced global transcriptional changes in the liver of these mice, we performed microarray analyses and conducted parametric analysis of gene set enrichment using these gene expression data and gene ontology gene sets. *Mogat1* inhibition suppressed several pathways composed of genes encoding proteins involved in fat synthesis, storage, and trafficking (Fig. 1*A*, *blue highlighted pathways*). As reported (13), many of these genes are known to be targets of PPARγ (*Cfd*, *Fsp27*, and *Plin4*) and SREBP1 (*Cidea* and *Elovl3*) (data not shown). Interestingly, pathway analysis of the regulated genes also suggested that a number of genes encoding markers of increased oxidative stress, chemokines, and inflammatory mediators were increased, rather than reduced, by *Mogat1* knockdown (Fig. 1*A*, *red highlighted pathways*). For example, glutathione *S*-transferase α1 (*Gsta1*) was significantly increased by *Mogat1* ASO (Fig. 1*B*). Serum amyloid A family (*Saa2* and *Saa3*) expression was increased by high fat diet feeding but further increased by *Mogat1* knockdown. Finally, expression of a number of chemokines (*Ccl2*, *Ccl5*, *Ccl7*, *Cxcl9*, and *Cxcl10*) and proinflammatory cytokines (*Il1a* and *Il1b*) were increased or tended to be increased by *Mogat1* inhibition. These findings suggest a disconnect between hepatic inflammation and metabolic improvements and suggest that the inflammation that occurs in response to this diet was actually accentuated by *Mogat1* inhibition.

Inhibition of Mogat1 Expression in Liver and Adipose Tissue Leads to Decreased Weight Gain and Adiposity—To properly examine the effects of *Mogat1* knockdown on hepatic inflammatory correlates of NASH, mice were fed a diet rich in trans fatty acids and fructose with supplemented cholesterol
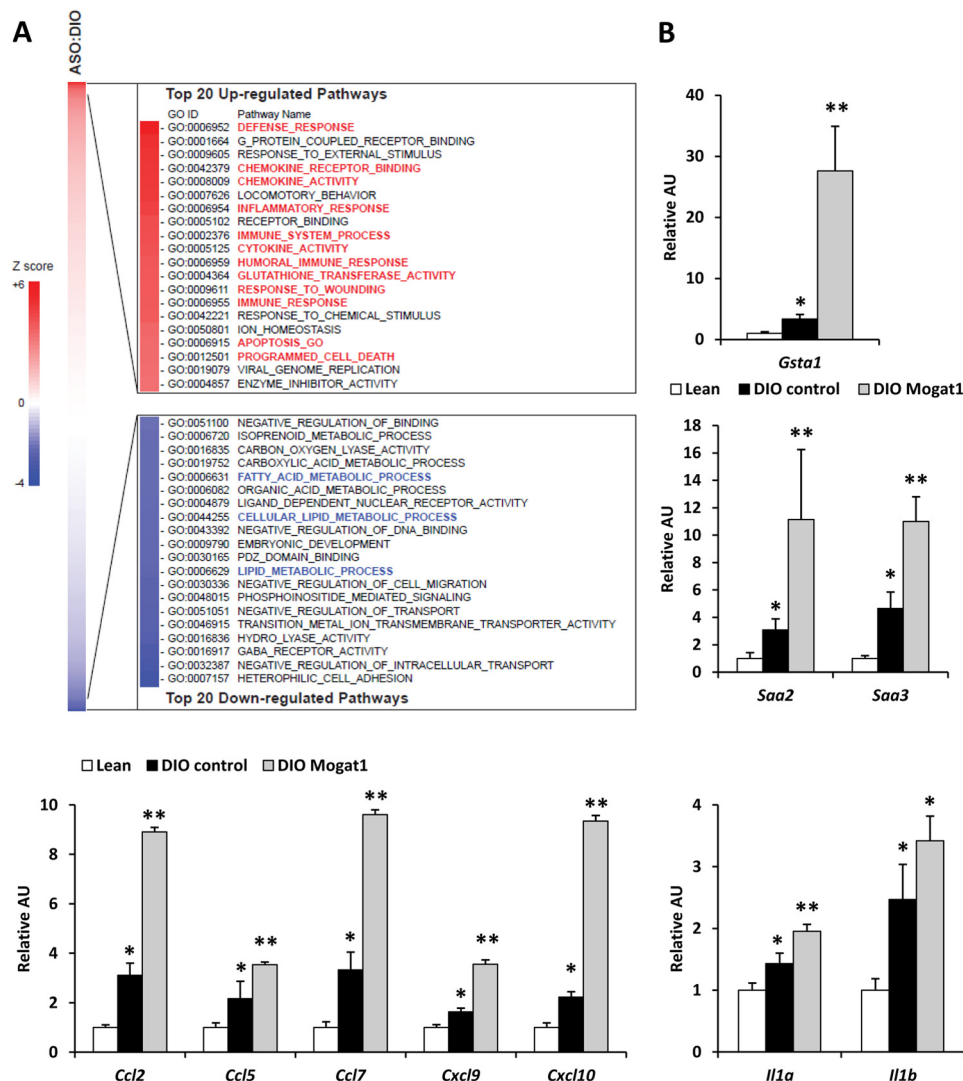
FIGURE 1. **Hepatic gene expression in DIO mice after *Mogat1* inhibition.** *A*, pathway analyses of hepatic gene expression array studies of DIO mice treated with control or *Mogat1* ASO. *B*, hepatic expression of the indicated genes in livers of lean and DIO mice treated with control or *Mogat1* ASOs. *, $p < 0.05$ *versus* lean controls; **, $p < 0.05$ *versus* lean and DIO controls. *Error bars*, S.E. *AU*, arbitrary units.

(HTF-C diet). Interestingly, the HTF-C diet was not obesogenic compared with the LF diet because weight gain of mice on LF and HTF-C diets injected with control ASO was not different (Fig. 2*A*). *Mogat1* ASO administration reduced weight gain compared with both the HTF-C and LF control ASO groups at weeks 13, 15, and 16 of the study (Fig. 2*A*). Decreased adiposity as evidenced by reduced fat pad weight of both the subcutaneous and epididymal fat compartments was noted (Fig. 2*B*).

Mogat1 Suppression Improved Glucose Tolerance—Glucose tolerance tests done after 10 weeks of ASO administration showed that HTF-C led to a significant worsening of glucose tolerance compared with LF controls in mice injected with control ASO (Fig. 2*C*), and *Mogat1* ASO treatment significantly improved glucose tolerance in HTF-C-fed mice (Fig. 2*C*). Insulin-stimulated Akt phosphorylation (Ser-473 and Thr-308), which was reduced in hepatocytes from mice fed HTF-C compared with LF diet, was increased by *Mogat1* knockdown (Fig. 2*D*). These data are consistent with our recent work showing that knocking down *Mogat1* in livers of mice fed a 60% fat diet

markedly improves glucose tolerance and hepatic insulin signaling (13).

Mogat1 Knockdown in Liver and Adipose Tissue Reduced Hepatic TAG Content—Consistent with our previous observations using a 60% fat diet, hepatic expression of *Mogat1* was increased in HTF-C diet-fed C57BL/6 mice compared with low fat (LF) diet controls (Fig. 3*A*). The HTF-C diet also tended to increase *Mogat2* expression. *Mogat1* ASO administration inhibited hepatic and epididymal adipose tissue *Mogat1* mRNA expression. The expression of *Mogat2* was not significantly affected by *Mogat1* ASO (Fig. 3*A*). *Mogat1* expression in the small intestine was not affected by *Mogat1* ASO (Fig. 3*A*). The HTF-C diet significantly increased liver weight and liver/body ratio compared with LF diet controls in mice treated with control ASO (Fig. 3*B*). *Mogat1* ASO treatment did not affect absolute liver weight or the liver weight/body weight ratio. A 6-fold increase in hepatic TAG content was detected in HTF-C compared with LF mice injected with control ASO (Fig. 3*C*). *Mogat1* ASO administration reduced hepatic TAG content compared with HTF-C
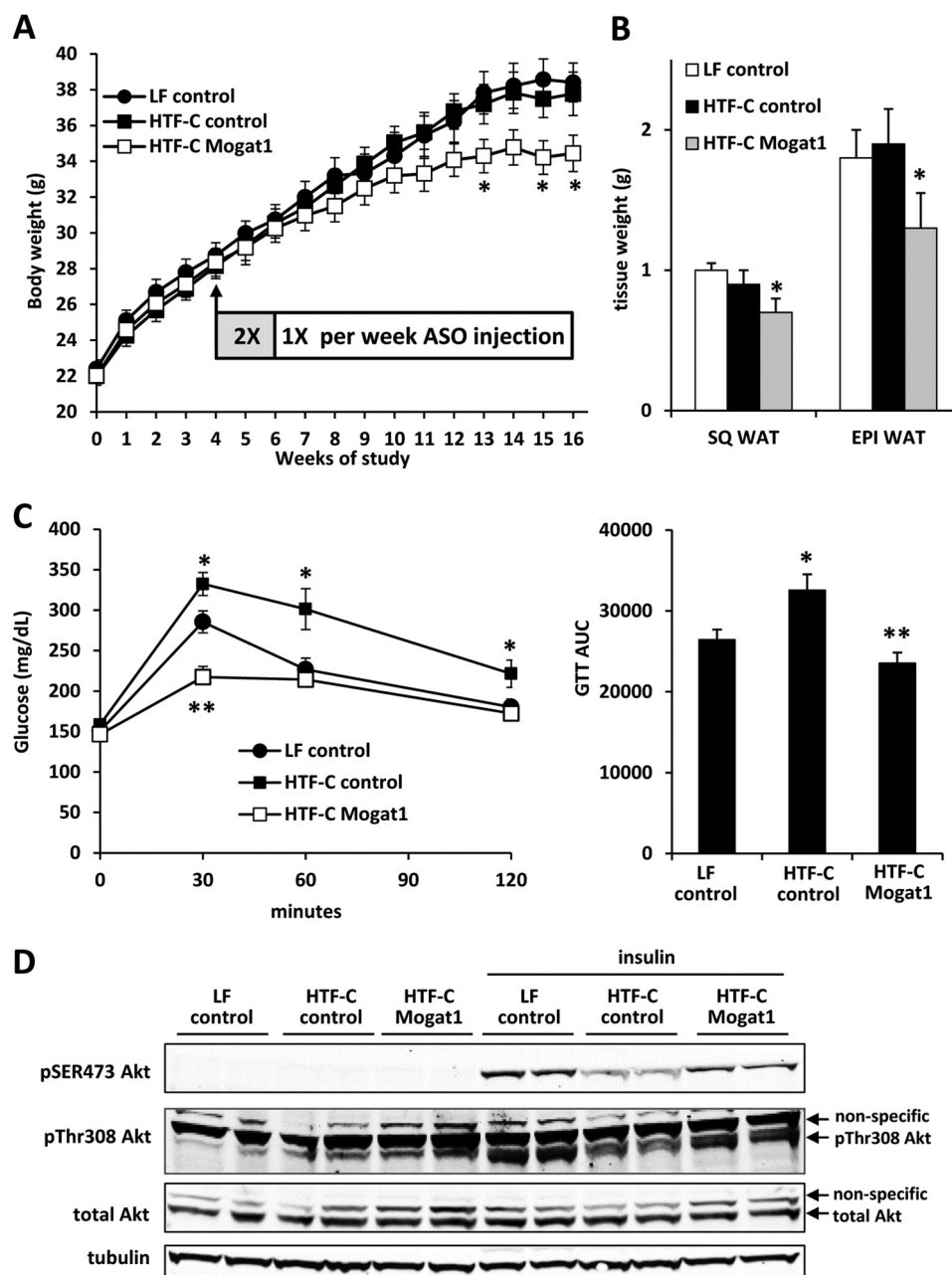
FIGURE 2. **Mogat1 ASO treatment improved glucose tolerance.** *A*, *Mogat1* inhibition led to decreased weight gain. *B*, reduced body weight after *Mogat1* inhibition is associated with diminished weight of subcutaneous (*SQ*) and epididymal (*EPI*) white adipose tissue (*WAT*) depots. *C*, results of GTT studies in mice fed an LF or HTF-C diet and treated with control or *Mogat1* ASOs. The bar graph at the *right* represents area under the curve values among the groups. $n = 10$ mice for all groups. *, $p < 0.05$ *versus* LF control and HTF-C *Mogat1*; **, $p < 0.05$ *versus* LF and HTF-C control. *D*, insulin-stimulated phosphorylation of Akt in hepatocytes isolated from mice treated with LF or HTF-C diet and control or *Mogat1* ASO. *Error bars*, S.E.

control mice, although TAG was still significantly increased compared with LF controls (Fig. 3*C*). Liver free cholesterol was increased in mice fed the HTF-C diet compared with the LF diet (Fig. 3*D*). However, there was no difference between the control and *Mogat1* ASO groups.

Mogat1 ASO Administration Failed to Reduce Hepatic DAG Content—Interestingly, hepatic content of the product of the reaction catalyzed by MGAT1, DAG, which was increased in the livers of HTF-C control mice compared with LF control mice, tended to be further increased by *Mogat1* ASO (Fig. 4*A*). Indeed, all species of DAG that were increased in HTF-C mice were unchanged by *Mogat1* inhibition (Fig. 4*B*). These included

DAG composed of saturated, monounsaturated, and polyunsaturated fatty acids. These findings are consistent with our recent work demonstrating that inhibition of *Mogat1* in mice fed a 60% fat diet did not reduce, but actually increased, hepatic DAG content (13). We also found that neither HTF-C diet nor *Mogat1* inhibition had an effect on total liver free fatty acid content (Fig. 4*C*). However, HTF-C diet significantly reduced the hepatic content of 14:0, 16:0, and 22:6 free fatty acids in liver (Fig. 7*D*), possibly reflecting a paucity of these fatty acid species in the diet. Neither HTF-C feeding nor *Mogat1* ASO treatment significantly affected plasma TAG, free fatty acids, or cholesterol concentrations (Table 2).
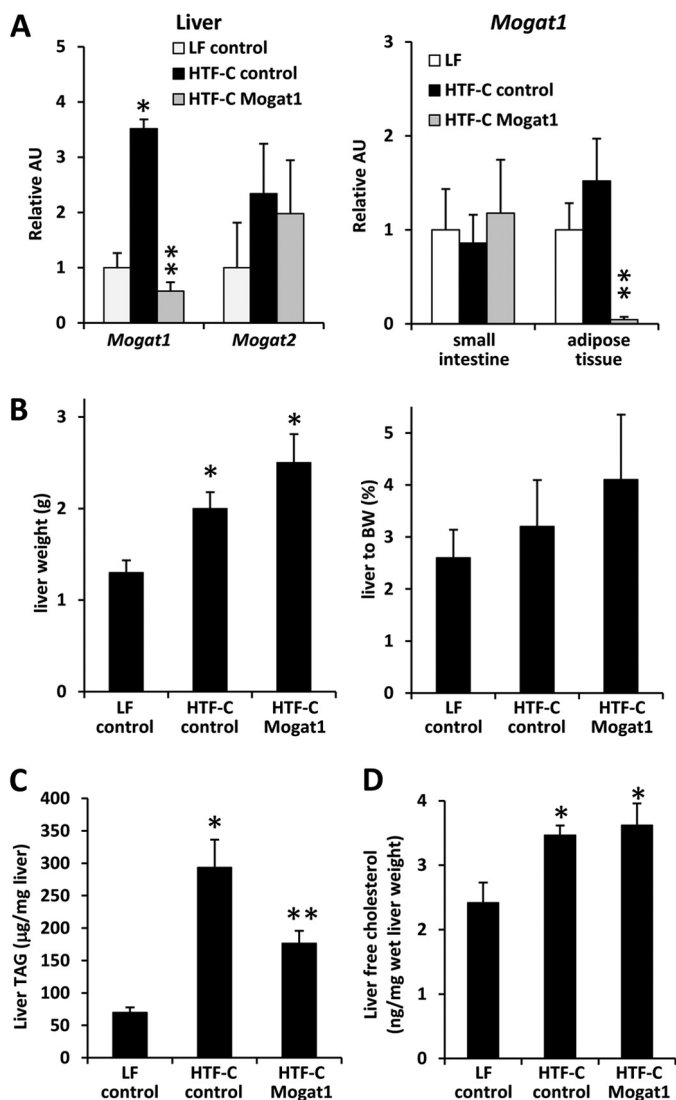
FIGURE 3. ***Mogat1* inhibition reduces hepatic TAG but not DAG content.** *A*, expression of *Mogat1* and *Mogat2* in the indicated tissues of mice fed LF or HTF-C diet and treated with control or *Mogat1* ASOs. *, $p < 0.05$ *versus* LF controls. **, $p < 0.05$ *versus* LF and HTF-C diet controls. *AU*, arbitrary units. *B*, liver weight and liver weight/body weight (*BW*) ratio. *, $p < 0.05$ *versus* LF controls. *C*, liver TAG content. Averages ± S.E. (*error bars*) for each group are shown. *, $p < 0.05$ *versus* LF controls. **, $p < 0.05$ *versus* both HTF-C and LF. *D*, liver free cholesterol content. *, $p < 0.05$ *versus* LF controls.

Increased Fatty Acid Oxidation and Reduced Lipogenesis following Mogat1 Knockdown—To evaluate the biochemical mechanism leading to reduced hepatic TAG content, we assessed rates of fatty acid oxidation, *de novo* lipogenesis, and TAG synthesis in hepatocytes of mice treated with LF or HTF-C diet with or without *Mogat1* knockdown. Rates of palmitate oxidation were significantly increased (Fig. 5*A*), whereas rates of fatty acid synthesis were significantly reduced (Fig. 5*B*), by *Mogat1* ASO treatment. Rates of TAG synthesis were increased in both HTF-C diet-fed groups compared with LF controls, and *Mogat1* ASO significantly reduced TAG synthetic rates in HTF-C hepatocytes (Fig. 5*C*). *Mogat1* ASO treatment was also associated with an increase in TG turnover in isolated hepatocytes (Fig. 5*C*).

To determine whether these metabolic changes were associated with altered expression of genes involved in these pro-

cesses, we measured the expression of genes encoding key enzymes in fatty acid oxidation, *de novo* lipogenesis, and TAG synthesis. We detected no significant effect of *Mogat1* ASO on the hepatic expression of fatty acid oxidation (*Cpt1a*, *Acadvl*, and *Acadm*), lipogenic (*Acaca*, *Fasn*), or TAG synthetic enzymes (*Lpin1*, *Lpin2*, and *Dgat1*) that was congruent with the metabolic effects observed in biochemical assays (Fig. 5*D*). The sole exception to this statement was that the expression of *Dgat2*, which acylates DAG to form TAG, was down-regulated by *Mogat1* ASO. This change correlates with decreased TAG synthesis rates and increased turnover.

Mogat1 ASO Fails to Prevent Liver Injury in Mice on HTF-C Diet—Inspection of histological liver sections from these mice did not grossly suggest any marked improvement in hepatic steatosis, injury, or leukocyte infiltration following *Mogat1* inhibition, although HTF-C clearly caused the accumulation of lipid droplets and accumulation of non-parenchymal cells (Fig. 6*A*). We examined this in a more detailed analysis by having a histopathologist, blinded to treatment group, evaluate the samples and generate a NAS. *Mogat1* inhibition did not improve any histological measures of steatohepatitis, including steatosis, hepatocyte ballooning, inflammation, or fibrosis grades in HTF-C-fed mice (Fig. 6*B*). Overall NAS, which was increased by HTF-C compared with LF in control ASO mice, was also not improved (Fig. 6*B*). Plasma AST and ALT levels were increased with HTF-C diet feeding and were not affected by *Mogat1* ASO treatment (Fig. 6*C*).

Mogat1 Inhibition Does Not Suppress Hepatic Expression of Gene Markers of Injury, Leukocyte Infiltration, or Stellate Cell Activation—Multiple cytokine and inflammatory markers that are commonly induced in NASH were up-regulated with the HTF-C diet. These included pro-inflammatory cytokines (*Tnfa*, *Il1a*, and *Il1b*), chemokines (*Ccl2*, *Ccl7*, *Cxcl1*, and *Cxcl10*), and macrophage cell surface markers (*Cd68* and *Cd11b*). There was no change in these markers with *Mogat1* ASO treatment, with the exception of *Ccl2* and *Cxcl10*, which were further induced by *Mogat1* ASO treatment (Fig. 7*A*). The expression of *Ccl5* and *Cxcl9* was also significantly increased by *Mogat1* ASO treatment. Although the majority of mice in the HTF-C control group failed to develop fibrosis histologically, the HTF-C diet induced expression of several genes involved in liver fibrogenesis and hepatic stellate cell activation, including *Col1a*, *Col3a*, *Timp1*, *Timp3*, *Mmp2*, *Fn1*, *Tgfb*, *Thbs*, and *Asma* (Fig. 7*B*). *Mogat1* inhibition in the liver did not alter the expression of these genes except that the HTF-C-induced increase in *Timp1* expression was significantly exacerbated in the *Mogat1* ASO group (Fig. 7*B*). Collectively, these data suggest that inhibition of *Mogat1* in mice fed the HTF-C diet improves glucose tolerance and reduces hepatic TAG content but does not suppress markers of liver inflammation or injury.

DISCUSSION

The accumulation of excessive or toxic species of lipids is believed to lead to hepatocyte injury and death, driving the development of NASH. The expression of the MGAT family of enzymes has recently been shown to be highly activated in the liver of several obese mouse models as well as in obese human
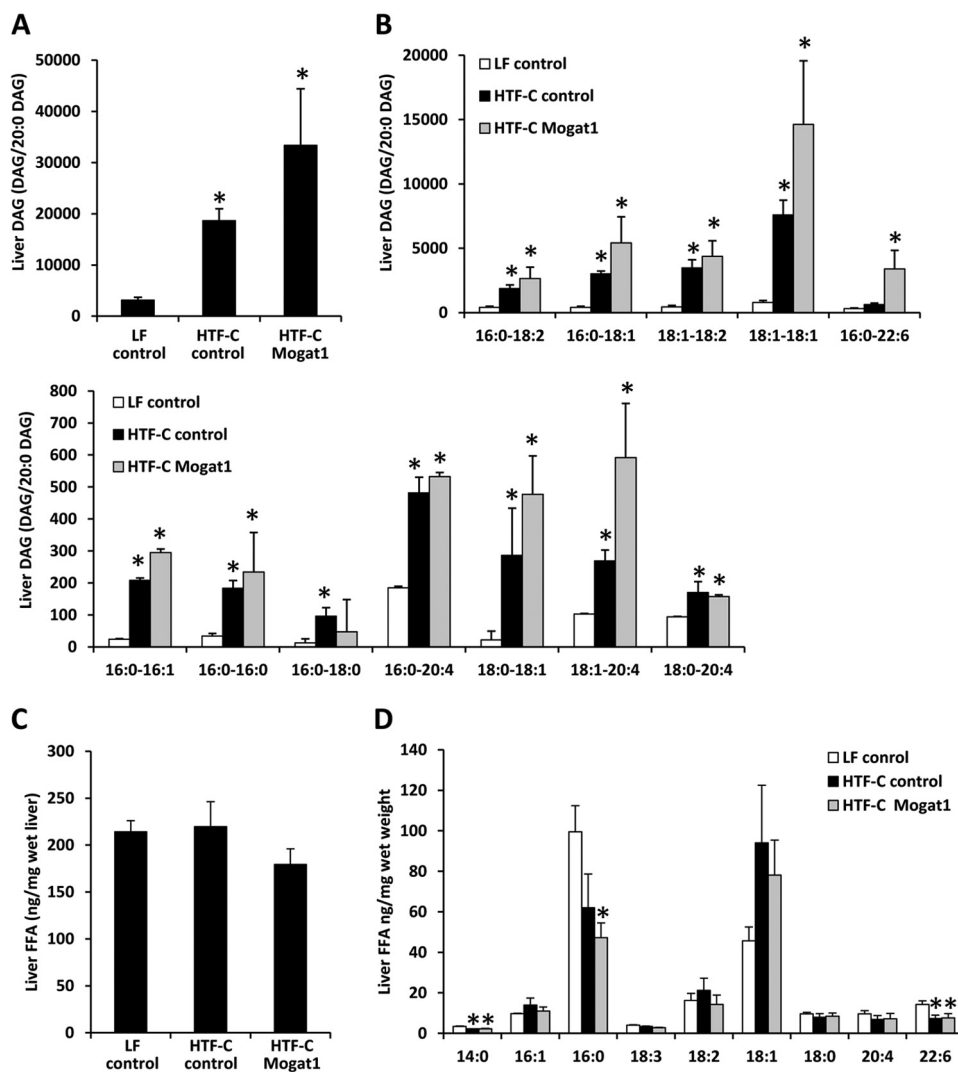
FIGURE 4. **Mogat1 inhibition does not affect liver DAG or free fatty acid content.** *A*, total liver DAG content. Averages ± S.E. (*error bars*) for each group are shown. Data shown are the ion intensity of the specified DAG molecular species normalized to the ion intensity of the internal standard 20:0 – 20:0 DAG/mg of tissue. *, $p < 0.05$ *versus* LF. *B*, liver DAG species by fatty acid chain length and saturation index. *C*, liver FFA content; *D*, FFA species. Averages ± S.E. for each group are shown. *, $p < 0.05$ *versus* LF.

TABLE 2

Plasma parameters

Plasma parameter	LF control	HTF-C control	HTF-C Mogat1
TAG (mg/dl)	109 ± 14	89 ± 10	91 ± 4
Cholesterol (mg/dl)	153 ± 9	174 ± 14	189 ± 20
FFA (mmol/liter)	0.6 ± 0.1	0.65 ± 0.1	0.5 ± 0.06

subjects (10, 12). Two recent studies have shown that inhibition of *Mogat1* in the liver improves hepatic and systemic metabolic indices (12, 13). However, from those studies, it was not clear whether liver inflammation and injury were also improved. Interestingly, although *Mogat1* inhibition reduced hepatic TAG content, enhanced fatty acid oxidation, reduced *de novo* lipogenesis, and markedly improved glucose tolerance in mice fed HTF-C diet, there was no beneficial effect on hepatic content or other lipids linked to liver injury, NASH indices, or gene expression markers for inflammation and fibrosis. Thus, improvements in glucose tolerance were surprisingly dissociated from corrections in DAG, free fatty acid, and cholesterol content as well as hepatic inflammatory end points, which have

previously been associated with hepatic metabolic abnormalities. These findings also suggest that improvements in metabolic parametes may be separable from the mechanisms that regulate the development of liver injury.

It is widely believed that reducing intrahepatic lipid content will have protective effects on the development of NASH. There are several examples of knock-out mice lacking key proteins involved in lipid synthesis (27) or storage (28 – 31) being protected from diet-induced hepatic steatosis. However, most of these studies showing beneficial effects detect a global reduction in intrahepatic lipid species, whereas we see a selective effect on TAG content without affecting other quantified lipids. Moreover, some work has suggested that inhibition of TAG synthesis is not necessarily beneficial toward these end points. For example, injections of ASOs against *Dgat2*, which catalyzes the step downstream of *Mogat1*, in mice on a methionine/choline-deficient diet were associated with worse liver fibrosis and apoptosis, despite a reduction in liver TAG content (32). In our study, decreased TAG content in the livers of mice that received
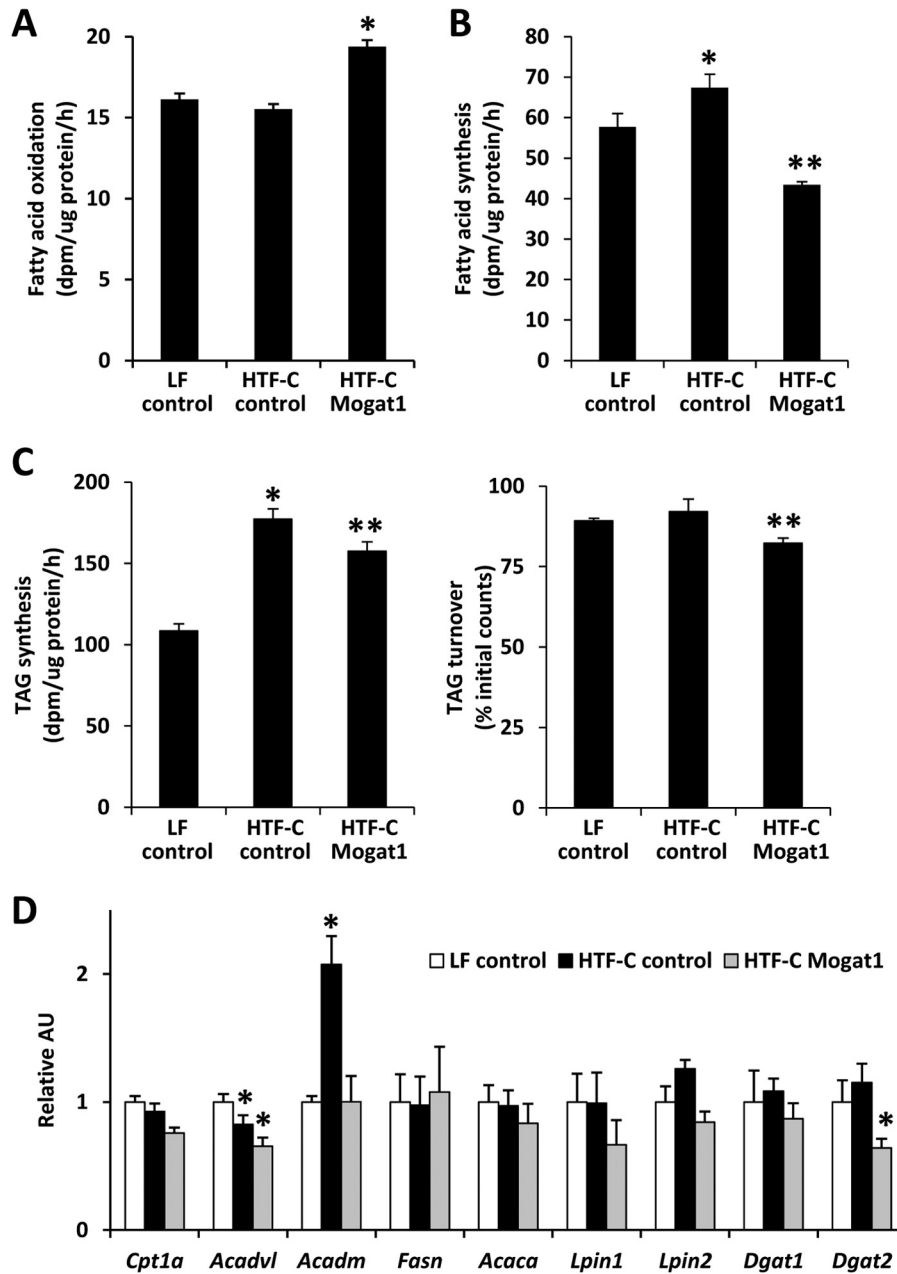
FIGURE 5. **Mogat1 ASO increases fatty acid oxidation and suppresses lipogenesis.** *A,* rates of hepatocyte palmitate oxidation. Averages $\pm$ S.E. (*error bars*) for each group are shown. *, $p < 0.05$ *versus* LF and HTF-C controls. *B,* rates of *de novo* lipogenesis. *, $p < 0.05$ *versus* LF controls. **, $p < 0.05$ *versus* LF and HTF-C controls. *C,* rates of triglyceride synthesis and turnover. *, $p < 0.05$ *versus* LF controls. **, $p < 0.05$ *versus* LF and HTF-C controls. *D,* expression of genes encoding fatty acid oxidation and lipogenic enzymes. *, $p < 0.05$ *versus* controls. *AU,* arbitrary units.

Mogat1 ASO on the HTF-C diet was not associated with improvement in inflammation, injury, or markers of fibrosis. TAG is probably not a pathogenic mediator in the development of NASH, and there may actually be a protective role of storing FFA in TAG. Hepatic free fatty acids and intermediates in the TAG synthesis pathway have been implicated in the pathology of NASH (33, 34). Impeding incorporation of FFA into TAG, the preferred and probably well buffered lipid storage form, could cause accumulation of other potentially toxic lipids, leading to hepatocyte injury or apoptosis. In this study, we found no increase in free fatty acid content of the liver with this diet. We also found dissociation between DAG and TAG accumulation, such that DAG levels remained high despite a reduction in

hepatic TAG. This DAG may be produced by the other, probably predominant, triglyceride synthesis pathway in an enzymatic step catalyzed by lipin family phosphatidate phosphohydrolases. We have shown previously that the accumulation of DAG in livers of mice with diminished MGAT activity is associated with deactivation of DGAT activity (13). *Mogat1* ASO also reduced *Dgat2* expression in this model, and we found that TAG turnover was increased, possibly due to reduced re-esterification of lipolytic products by DGAT and MGAT. Congruent with this, *Mogat1* knockdown increased rates of palmitate oxidation independent of changes in the expression of oxidative enzymes, suggesting that more of the intrahepatic fat was directed toward an oxidative fate. Finally, rates of *de novo* lipo-
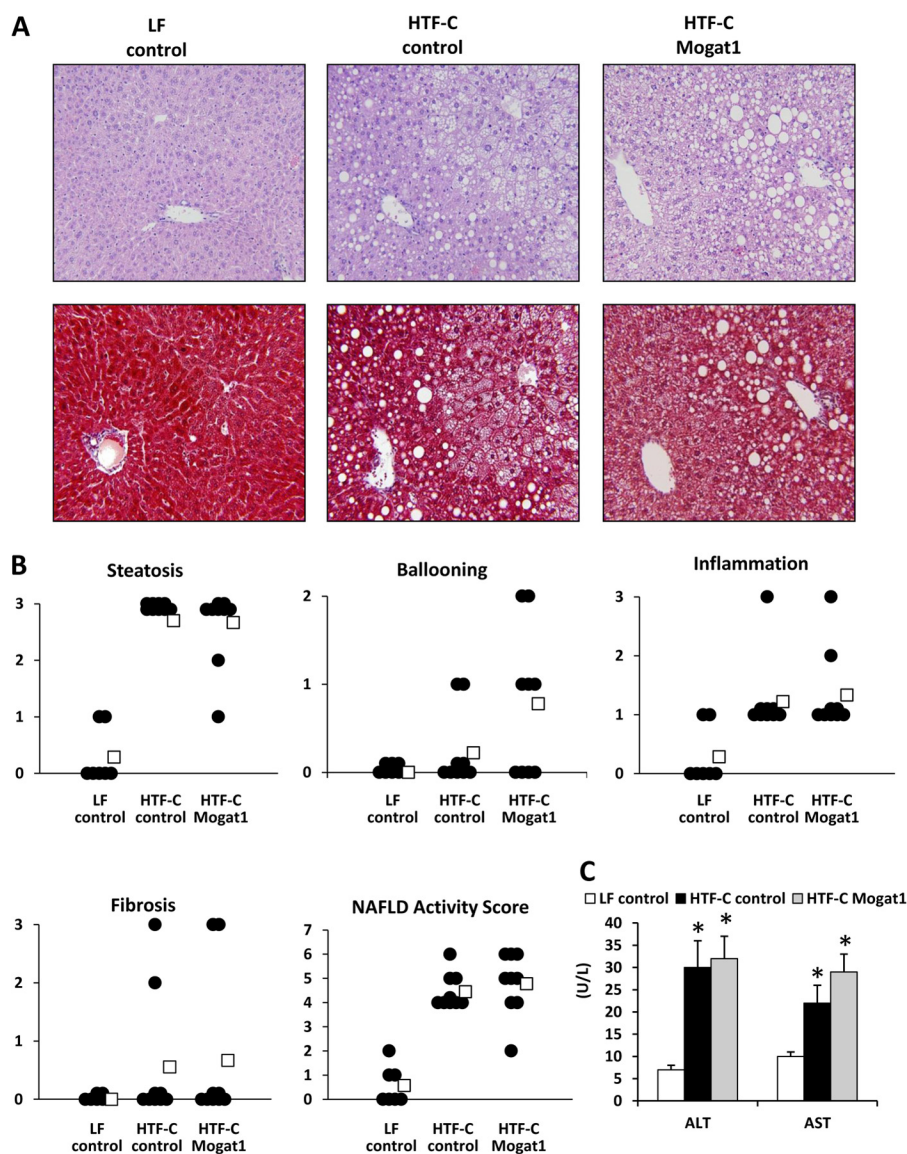
FIGURE 6. **Hepatic *Mogat1* inhibition does not result in histological improvement of steatohepatitis.** *A*, H&E- and trichrome-stained liver sections from mice fed an LF or HTF-C diet and treated with control or *Mogat1* ASOs. *B*, graphs depict results of NAS by a histopathologist blinded to treatment group. Data points represent individual mice, and averages (*open boxes*) for each group are also shown. Steatosis grading was done on low to medium power evaluation of parenchymal involvement by steatosis (0 for <5%, 1 for 5–33%, 2 for 33–66%, and 3 for more than 66%). Inflammation was graded by overall assessment of all inflammatory foci on a ×200 field (0 for no foci, 1 for <2, 2 for 2–4 foci, and 3 for >4 foci). Ballooning score was 0 for no ballooned cells per field, 1 for few, and 2 for many. Fibrosis was graded 0 for no fibrosis, 1 for perisinusoidal or periportal/portal, 2 for perisinusoidal and periportal/portal, 3 for bridging fibrosis, and 4 for cirrhosis. NAS is the sum of steatosis, inflammation, and ballooning scores. *C*, plasma ALT and AST concentrations are shown. *U/L*, units/liter. *, $p < 0.05$ *versus* LF. *Error bars*, S.E.

genesis were reduced by *Mogat* knockdown. Whether these metabolic effects are a cause or consequence of the metabolic improvements is not clear, and the specific lipid or classes of lipids that mediate liver injury in this and other models of NASH remain to be clarified.

Typical rodent high fat diets employed to cause obesity and produce hepatic steatosis are usually not associated with development of severe liver inflammation and fibrosis in mice unless they are fed for extremely long durations. In the past few years, attempts have been made to induce liver injury by using a number of permutations of the high fat diet formula (35) and/or by superimposing other insults with the dietary regimen (36–41). Studies utilizing a combination of high fat diets containing high levels of trans fatty acids, often in combination with increased

dietary fructose or the addition of cholesterol have enjoyed success at provoking liver injury (15, 42, 43). In the present study, we employed one of these previously used diets (15) and found that hepatocyte ballooning and other histologic indices of NASH were increased by feeding this diet for 16 weeks. Furthermore, several gene expression markers for leukocyte infiltration, inflammation, and stellate cell activation were elevated. However, histologic scoring of liver sections and hydroxyproline assays (data not shown) failed to detect fibrosis in the majority of the mice in this study. Also, compared with LF control diet mice, HTF-C diet-fed mice were not more obese. It is possible that the purified LF diet, which contains supplemented glucose, is very palatable, causing the control mice to overeat because the body weight of the LF control mice was quite high
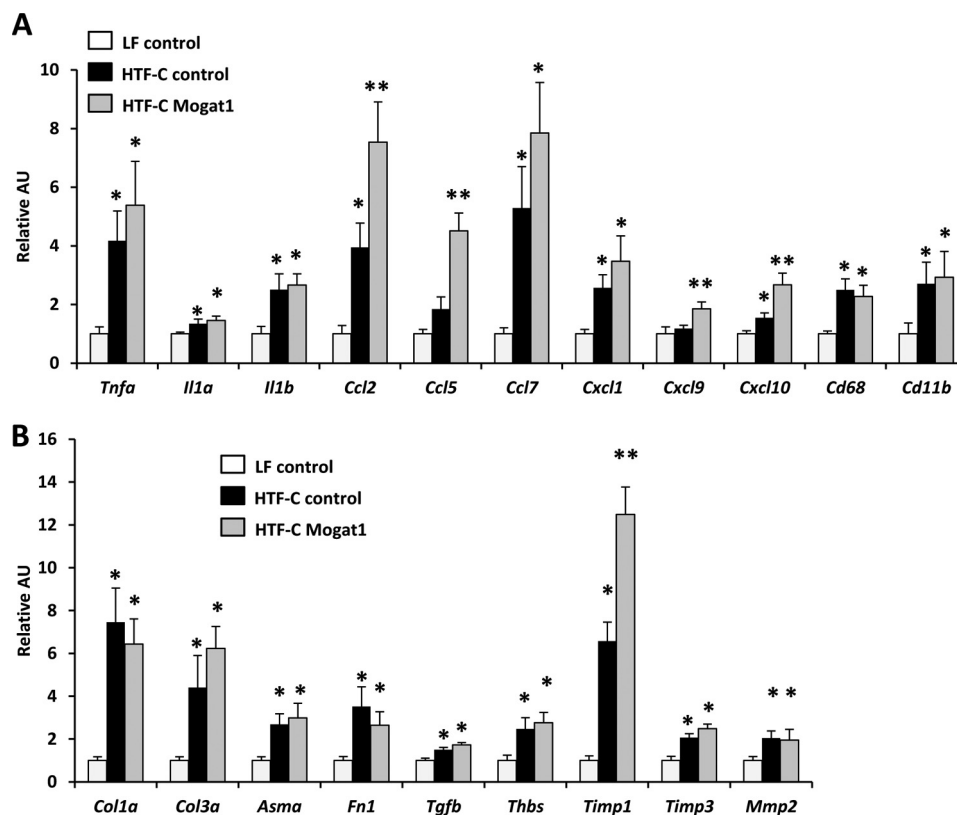
FIGURE 7. **Gene expression markers for liver injury, inflammation, and NASH.** Hepatic expression of inflammatory and cytokine markers (*A*) and fibrogenic and hepatic stellate cell activation markers (*B*) in livers of mice fed an LF or HTF-C diet and treated with control or *Mogat1* ASOs. *, $p < 0.05$ *versus* LF; **, $p < 0.05$ *versus* both HTF-C and LF. *Error bars*, S.E. *AU*, arbitrary units.

for mice of the C57BL/6 strain at this age. Nonetheless, HTF-C diet causes glucose intolerance, hepatic steatosis, and liver inflammation and injury, despite the lack of effect on body weight.

Although not a perfect model of human NASH, there are a number of aspects to this diet that make it attractive for testing hypotheses regarding the utility of novel therapeutics for NASH. For example, our previous work with inhibition of *Mogat1* in mice on a 60% fat diet also showed marked improvements in hepatic insulin signaling and systemic glycemia (13). However, we were unable to assess the effects on liver injury because that diet provokes relatively little inflammation or injury. A methionine/choline-deficient diet is associated with weight loss and increased insulin sensitivity (44, 45) and is not a faithful model for NASH in the setting of overnutrition. Our previous work, with the present study, suggests that inhibiting MGAT activity may be an effective insulin-sensitizing therapy but that this may not reduce clinical measures of NASH. The present data illustrate the need for careful assessment of potential adverse outcomes of MGAT inhibition in what might seem to be a promising therapeutic target for metabolic syndrome.

In conclusion, the current study demonstrated that inhibiting hepatic *Mogat1* in a mouse model of NASH reduces weight gain, hepatic TAG content, and glucose tolerance but does not improve inflammation, injury, or markers of NASH. It may be worthwhile to re-examine these findings in other mouse models of NASH and by using other methods to inhibit MGAT activity. Additional work on inhibiting other members of the

MGAT family as well as the development of mice with liver-specific knockout of these genes could help shed more light on the role of the MGAT pathway in metabolic abnormalities, simple hepatic steatosis, and NASH.

REFERENCES

1. Vernon, G., Baranova, A., and Younossi, Z. M. (2011) Systematic review: the epidemiology and natural history of non-alcoholic fatty liver disease and non-alcoholic steatohepatitis in adults. *Aliment. Pharmacol. Ther.* **34,** 274–285
2. Fan, J. G., and Cao, H. X. (2013) Role of diet and nutritional management in non-alcoholic fatty liver disease. *J. Gastroenterol. Hepatol.* **28,** 81–87
3. Sookoian, S., and Pirola, C. J. (2011) Meta-analysis of the influence of I148M variant of patatin-like phospholipase domain containing 3 gene (PNPLA3) on the susceptibility and histological severity of nonalcoholic fatty liver disease. *Hepatology* **53,** 1883–1894
4. Zhu, L., Baker, S. S., Gill, C., Liu, W., Alkhouri, R., Baker, R. D., and Gill, S. R. (2013) Characterization of gut microbiomes in nonalcoholic steatohepatitis (NASH) patients: a connection between endogenous alcohol and NASH. *Hepatology* **57,** 601–609
5. Yue, Y. G., Chen, Y. Q., Zhang, Y., Wang, H., Qian, Y. W., Arnold, J. S., Calley, J. N., Li, S. D., Perry, W. L., 3rd, Zhang, H. Y., Konrad, R. J., and Cao, G. (2011) The acyl coenzyme A:monoacylglycerol acyltransferase 3 (MGAT3) gene is a pseudogene in mice but encodes a functional enzyme in rats. *Lipids* **46,** 513–520
6. Cao, J., Cheng, L., and Shi, Y. (2007) Catalytic properties of MGAT3, a putative triacylglycerol synthase. *J. Lipid Res.* **48,** 583–591

7. Shi, Y., and Cheng, D. (2009) Beyond triglyceride synthesis: the dynamic functional roles of MGAT and DGAT enzymes in energy metabolism. *Am. J. Physiol. Endocrinol. Metab.* **297,** E10–E18

8. Xia, T., Mostafa, N., Bhat, B. G., Florant, G. L., and Coleman, R. A. (1993) Selective retention of essential fatty acids: the role of hepatic monoacylglycerol acyltransferase. *Am. J. Physiol.* **265,** R414–R419

9. Bhat, B. G., Wang, P., and Coleman, R. A. (1994) Hepatic monoacylglycerol acyltransferase is regulated by *sn*-1,2-diacylglycerol and by specific lipids in Triton X-100/phospholipid-mixed micelles. *J. Biol. Chem.* **269,** 13172–13178

10. Hall, A. M., Kou, K., Chen, Z., Pietka, T. A., Kumar, M., Korenblat, K. M., Lee, K., Ahn, K., Fabbrini, E., Klein, S., Goodwin, B., and Finck, B. N. (2012) Evidence for regulated monoacylglycerol acyltransferase expression and activity in human liver. *J. Lipid Res.* **53,** 990–999

11. Cortés, V. A., Curtis, D. E., Sukumaran, S., Shao, X., Parameswara, V., Rashid, S., Smith, A. R., Ren, J., Esser, V., Hammer, R. E., Agarwal, A. K., Horton, J. D., and Garg, A. (2009) Molecular mechanisms of hepatic steatosis and insulin resistance in the AGPAT2-deficient mouse model of congenital generalized lipodystrophy. *Cell Metab.* **9,** 165–176

12. Lee, Y. J., Ko, E. H., Kim, J. E., Kim, E., Lee, H., Choi, H., Yu, J. H., Kim, H. J., Seong, J. K., Kim, K. S., and Kim, J. W. (2012) Nuclear receptor PPARγ-regulated monoacylglycerol *O*-acyltransferase 1 (MGAT1) expression is responsible for the lipid accumulation in diet-induced hepatic steatosis. *Proc. Natl. Acad. Sci. U.S.A.* **109,** 13656–13661

13. Hall, A. M., Soufi, N., Chambers, K. T., Chen, Z., Schweitzer, G. G., McCommis, K. S., Erion, D. M., Graham, M. J., Su, X., and Finck, B. N. (2014) Abrogating monoacylglycerol acyltransferase activity in liver improves glucose tolerance and hepatic insulin signaling in obese mice. *Diabetes* **63,** 2284–2296

14. Clapper, J. R., Hendricks, M. D., Gu, G., Wittmer, C., Dolman, C. S., Herich, J., Athanacio, J., Villescaz, C., Ghosh, S. S., Heilig, J. S., Lowe, C., and Roth, J. D. (2013) Diet-induced mouse model of fatty liver disease and nonalcoholic steatohepatitis reflecting clinical disease progression and methods of assessment. *Am. J. Physiol. Gastrointest. Liver Physiol.* **305,** G483–G495

15. Trevaskis, J. L., Griffin, P. S., Wittmer, C., Neuschwander-Tetri, B. A., Brunt, E. M., Dolman, C. S., Erickson, M. R., Napora, J., Parkes, D. G., and Roth, J. D. (2012) Glucagon-like peptide-1 receptor agonism improves metabolic, biochemical, and histopathological indices of nonalcoholic steatohepatitis in mice. *Am. J. Physiol. Gastrointest. Liver Physiol.* **302,** G762–G772

16. Chen, Z., Gropler, M. C., Norris, J., Lawrence, J. C., Jr., Harris, T. E., and Finck, B. N. (2008) Alterations in hepatic metabolism in fld mice reveal a role for lipin 1 in regulating VLDL-triacylglyceride secretion. *Arterioscler. Thromb. Vasc. Biol.* **28,** 1738–1744

17. Burgess, S. C., Leone, T. C., Wende, A. R., Croce, M. A., Chen, Z., Sherry, A. D., Malloy, C. R., and Finck, B. N. (2006) Diminished hepatic gluconeogenesis via defects in tricarboxylic acid cycle flux in peroxisome proliferator-activated receptor γ coactivator-1α (PGC-1α)-deficient mice. *J. Biol. Chem.* **281,** 19000–19008

18. Lin, X., Schonfeld, G., Yue, P., and Chen, Z. (2002) Hepatic fatty acid synthesis is suppressed in mice with fatty livers due to targeted apolipoprotein B38.9 mutation. *Arterioscler. Thromb. Vasc. Biol.* **22,** 476–482

19. Chen, Z., Norris, J. Y., and Finck, B. N. (2010) Peroxisome proliferator-activated receptor-γ coactivator-1α (PGC-1α) stimulates VLDL assembly through activation of cell death-inducing DFFA-like effector B (CideB). *J. Biol. Chem.* **285,** 25996–26004

20. Kim, S. Y., and Volsky, D. J. (2005) PAGE: parametric analysis of gene set enrichment. *BMC Bioinformatics* **6,** 144

21. Yoshino, J., Mills, K. F., Yoon, M. J., and Imai, S. (2011) Nicotinamide mononucleotide, a key NAD+ intermediate, treats the pathophysiology of diet- and age-induced diabetes in mice. *Cell Metab.* **14,** 528–536

22. Hjelkrem, M., Stauch, C., Shaw, J., and Harrison, S. A. (2011) Validation of the non-alcoholic fatty liver disease activity score. *Aliment. Pharmacol. Ther.* **34,** 214–218

23. Kleiner, D. E., Brunt, E. M., Van Natta, M., Behling, C., Contos, M. J., Cummings, O. W., Ferrell, L. D., Liu, Y. C., Torbenson, M. S., Unalp-Arida, A., Yeh, M., McCullough, A. J., Sanyal, A. J., and Nonalcoholic

Steatohepatitis Clinical Research Network (2005) Design and validation of a histological scoring system for nonalcoholic fatty liver disease. *Hepatology* **41,** 1313–1321

24. Bowden, J. A., Albert, C. J., Barnaby, O. S., and Ford, D. A. (2011) Analysis of cholesteryl esters and diacylglycerols using lithiated adducts and electrospray ionization-tandem mass spectrometry. *Anal. Biochem.* **417,** 202–210

25. Brown, R. J., Shao, F., Baldán, A., Albert, C. J., and Ford, D. A. (2013) Cholesterol efflux analyses using stable isotopes and mass spectrometry. *Anal. Biochem.* **433,** 56–64

26. Yang, Y., Kuwano, T., Lagor, W. R., Albert, C. J., Brenton, S., Rader, D. J., Ford, D. A., and Brown, R. J. (2014) Lipidomic analyses of female mice lacking hepatic lipase and endothelial lipase indicate selective modulation of plasma lipid species. *Lipids* **49,** 505–515

27. Hammond, L. E., Gallagher, P. A., Wang, S., Hiller, S., Kluckman, K. D., Posey-Marcos, E. L., Maeda, N., and Coleman, R. A. (2002) Mitochondrial glycerol-3-phosphate acyltransferase-deficient mice have reduced weight and liver triacylglycerol content and altered glycerolipid fatty acid composition. *Mol. Cell. Biol.* **22,** 8204–8214

28. Chang, B. H., Li, L., Paul, A., Taniguchi, S., Nannegari, V., Heird, W. C., and Chan, L. (2006) Protection against fatty liver but normal adipogenesis in mice lacking adipose differentiation-related protein. *Mol. Cell. Biol.* **26,** 1063–1076

29. McManaman, J. L., Bales, E. S., Orlicky, D. J., Jackman, M., MacLean, P. S., Cain, S., Crunk, A. E., Mansur, A., Graham, C. E., Bowman, T. A., and Greenberg, A. S. (2013) Perilipin-2-null mice are protected against diet-induced obesity, adipose inflammation, and fatty liver disease. *J. Lipid Res.* **54,** 1346–1359

30. Zhou, L., Xu, L., Ye, J., Li, D., Wang, W., Li, X., Wu, L., Wang, H., Guan, F., and Li, P. (2012) Cidea promotes hepatic steatosis by sensing dietary fatty acids. *Hepatology* **56,** 95–107

31. Li, J. Z., Ye, J., Xue, B., Qi, J., Zhang, J., Zhou, Z., Li, Q., Wen, Z., and Li, P. (2007) Cideb regulates diet-induced obesity, liver steatosis, and insulin sensitivity by controlling lipogenesis and fatty acid oxidation. *Diabetes* **56,** 2523–2532

32. Yamaguchi, K., Yang, L., McCall, S., Huang, J., Yu, X. X., Pandey, S. K., Bhanot, S., Monia, B. P., Li, Y. X., and Diehl, A. M. (2007) Inhibiting triglyceride synthesis improves hepatic steatosis but exacerbates liver damage and fibrosis in obese mice with nonalcoholic steatohepatitis. *Hepatology* **45,** 1366–1374

33. Anderson, N., and Borlak, J. (2008) Molecular mechanisms and therapeutic targets in steatosis and steatohepatitis. *Pharmacol. Rev.* **60,** 311–357

34. Cheung, O., and Sanyal, A. J. (2008) Abnormalities of lipid metabolism in nonalcoholic fatty liver disease. *Semin. Liver Dis.* **28,** 351–359

35. Nagarajan, P., Mahesh Kumar, M. J., Venkatesan, R., Majundar, S. S., and Juyal, R. C. (2012) Genetically modified mouse models for the study of nonalcoholic fatty liver disease. *World J. Gastroenterol.* **18,** 1141–1153

36. Kubota, N., Kado, S., Kano, M., Masuoka, N., Nagata, Y., Kobayashi, T., Miyazaki, K., and Ishikawa, F. (2013) A high-fat diet and multiple administration of carbon tetrachloride induces liver injury and pathological features associated with non-alcoholic steatohepatitis in mice. *Clin. Exp. Pharmacol. Physiol.* **40,** 422–430

37. Kita, Y., Takamura, T., Misu, H., Ota, T., Kurita, S., Takeshita, Y., Uno, M., Matsuzawa-Nagata, N., Kato, K., Ando, H., Fujimura, A., Hayashi, K., Kimura, T., Ni, Y., Otoda, T., Miyamoto, K., Zen, Y., Nakanuma, Y., and Kaneko, S. (2012) Metformin prevents and reverses inflammation in a non-diabetic mouse model of nonalcoholic steatohepatitis. *PloS One* **7,** e43056

38. Fukunishi, S., Nishio, H., Fukuda, A., Takeshita, A., Hanafusa, T., Higuchi, K., and Suzuki, K. (2009) Development of fibrosis in nonalcoholic steatosis through combination of a synthetic diet rich in disaccharide and low-dose lipopolysaccharides in the livers of Zucker (fa/fa) rats. *J. Clin. Biochem. Nutr.* **45,** 322–328

39. Yang, S. Q., Lin, H. Z., Lane, M. D., Clemens, M., and Diehl, A. M. (1997) Obesity increases sensitivity to endotoxin liver injury: implications for the pathogenesis of steatohepatitis. *Proc. Natl. Acad. Sci. U. S. A.* **94,** 2557–2562

40. Sato, W., Horie, Y., Kataoka, E., Ohshima, S., Dohmen, T., Iizuka, M., Sasaki, J., Sasaki, T., Hamada, K., Kishimoto, H., Suzuki, A., and Watanabe,

S. (2006) Hepatic gene expression in hepatocyte-specific Pten deficient mice showing steatohepatitis without ethanol challenge. *Hepatol. Res.* **34,** 256–265

41. Svegliati-Baroni, G., Candelaresi, C., Saccomanno, S., Ferretti, G., Bachetti, T., Marzioni, M., De Minicis, S., Nobili, L., Salzano, R., Omenetti, A., Pacetti, D., Sigmund, S., Benedetti, A., and Casini, A. (2006) A model of insulin resistance and nonalcoholic steatohepatitis in rats: role of peroxisome proliferator-activated receptor-α and *n*-3 polyunsaturated fatty acid treatment on liver injury. *Am. J. Pathol.* **169,** 846–860

42. Kohli, R., Kirby, M., Xanthakos, S. A., Softic, S., Feldstein, A. E., Saxena, V., Tang, P. H., Miles, L., Miles, M. V., Balistreri, W. F., Woods, S. C., and Seeley, R. J. (2010) High-fructose, medium chain trans fat diet induces liver fibrosis and elevates plasma coenzyme Q9 in a novel murine model of obesity and nonalcoholic steatohepatitis. *Hepatology* **52,** 934–944

43. Matsuzawa, N., Takamura, T., Kurita, S., Misu, H., Ota, T., Ando, H., Yokoyama, M., Honda, M., Zen, Y., Nakanuma, Y., Miyamoto, K., and Kaneko, S. (2007) Lipid-induced oxidative stress causes steatohepatitis in mice fed an atherogenic diet. *Hepatology* **46,** 1392–1403

44. Rinella, M. E., and Green, R. M. (2004) The methionine-choline deficient dietary model of steatohepatitis does not exhibit insulin resistance. *J. Hepatol.* **40,** 47–51

45. Rizki, G., Arnaboldi, L., Gabrielli, B., Yan, J., Lee, G. S., Ng, R. K., Turner, S. M., Badger, T. M., Pitas, R. E., and Maher, J. J. (2006) Mice fed a lipogenic methionine-choline-deficient diet develop hypermetabolism coincident with hepatic suppression of SCD-1. *J. Lipid Res.* **47,** 2280–2290